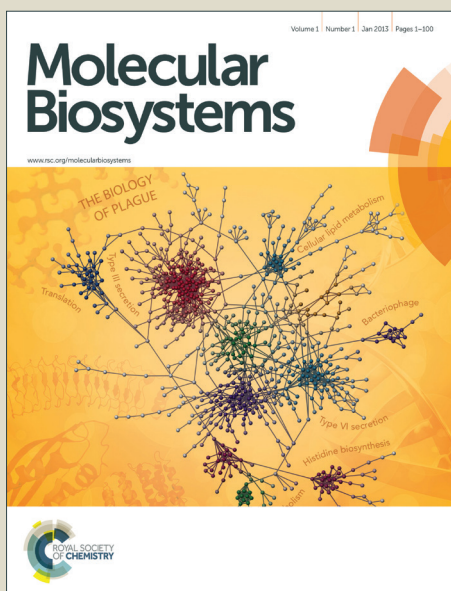


Molecular BioSystems

Accepted Manuscript



This is an *Accepted Manuscript*, which has been through the Royal Society of Chemistry peer review process and has been accepted for publication.

Accepted Manuscripts are published online shortly after acceptance, before technical editing, formatting and proof reading. Using this free service, authors can make their results available to the community, in citable form, before we publish the edited article. We will replace this *Accepted Manuscript* with the edited and formatted *Advance Article* as soon as it is available.

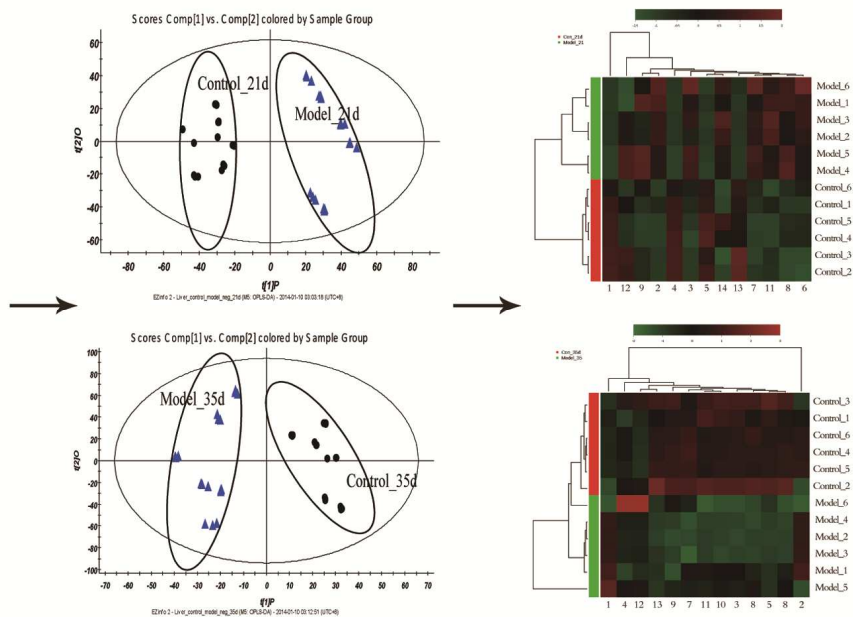
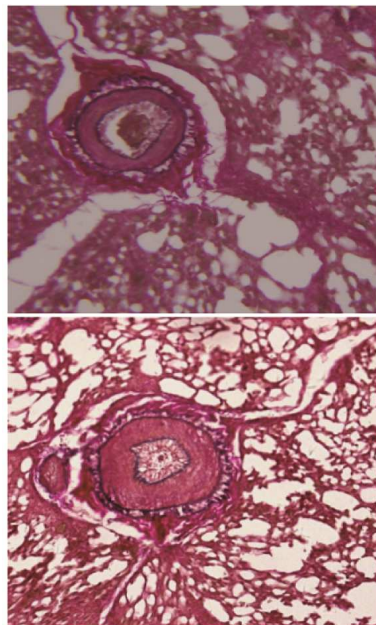
You can find more information about *Accepted Manuscripts* in the [Information for Authors](#).

Please note that technical editing may introduce minor changes to the text and/or graphics, which may alter content. The journal's standard [Terms & Conditions](#) and the [Ethical guidelines](#) still apply. In no event shall the Royal Society of Chemistry be held responsible for any errors or omissions in this *Accepted Manuscript* or any consequences arising from the use of any information it contains.



www.rsc.org/molecularbiosystems

Contents entry



Text: Hepatic metabolomic profiles of low-temperature induced ascites syndrome showed disturbances on the metabolism of bile acids and phospholipid

Metabolomics analysis reveals that bile acids and phospholipids contribute to variable responses to low-temperature-induced ascites syndrome

Yiru Shen,^{a,1} Shourong Shi,^{a,b,1} Haibing Tong,^a Yuming Guo,^{b,*} and Jianmin Zou,^{a,*}

Ascites is a major problem for both human health and animal production, due to its association with high rates of morbidity and mortality, low efficiency of nutrients utilization, and permanent adverse effects on performance. Although it is one of the three major metabolic diseases in poultry production, the underlying mechanisms are largely unknown. In this study, six ascites syndrome (AS) chickens and six normal chickens were obtained from each group (108 chickens) at 21 and 35 days. A liver metabolomics method based on ultra-performance liquid chromatography/quadrupole time-of-flight mass spectrometry (UPLC/Q-TOF/MS) was used to explore the metabolic pattern of low molecular mass metabolites in chickens with low-temperature-induced AS. Coupled with blood biochemistry and histopathology results, the significant difference in metabolic profiling between the AS group and the control group, as determined through pattern recognition analysis, indicated changes in global tissue metabolites. The results showed that a primary bile acids synthesis disorder and inflammation had occurred by 21 days and that lysophospholipid metabolism was disrupted by 35 days with the continuation of low temperatures. Several metabolites, including taurodeoxycholic acid, cholic acid glucuronide, glycocholic acid, LysoPC(15:0) and taurocholic acid, were identified as the potential and proper biomarkers of AS. These biochemical changes in tissue metabolites are related to perturbations of lipid metabolism, which may be helpful to further understand the AS mechanisms. This work shows that the metabolomics is a valuable tool for studying metabolic diseases.

Introduction

Ascites, which commonly occurs in vertebrates, is a major problem for both human health and animal production. Ascites is the most common of the three major complications of cirrhosis, and many patients are referred for liver transplantation after the development of ascites.¹ Ascites, a serious metabolic disease, overwhelmed approximately 50% of patients in two years.² Meat-type chickens are sensitive to ascites syndrome (AS) due to intensive

genetic selection for rapid growth and exposure to extreme environmental conditions and nutritional levels such as low temperatures, high altitudes or high energy diets.³ As one of three major metabolic diseases, AS causes considerable economic losses in poultry production. AS mortality generally occurs late in the broiler production process, with a peak occurring by 39 days, and ascetic birds are rejected for consumption {Broadhurst, 2006 #6}.⁴ Moreover, AS is a severe animal welfare problem because the symptoms, which include breathing difficulties, are progressive and distressing.^{5,6} AS in broiler chickens is usually the result of chronic passive congestion (increased pressure in the splanchnic venous system, particularly the liver) caused by right ventricular failure.⁷ It is also the result of liver damage. Liver damage that interferes with venous return and portal hypertension has been reported to cause pulmonary hypertension in rats and humans, although the mechanism is not understood.⁸

Knowledge of the complex molecular and pathophysiological mechanisms leading to AS remains limited, in part because conventional

^aPoultry Institute, Chinese Academy of Agricultural Sciences, Yangzhou Jiangsu 225125, China

^b State Key Laboratory of Animal Nutrition, Department of Animal Science and Technology, China Agricultural University, Beijing 100093, China

To whom correspondence should be addressed: Jianmin Zou, Tel.: +86-514-85599001, Fax, +86-514-85599035; E-mail: jqszejm@163.com; Y. M. Guo: Tel, +86-10-62733900; Fax, +86-10-62733900; E-mail: guoym@aliyun.com;

research tools have hampered investigators by restricting their focus to a single or a relatively limited number of risk markers at one time. Metabolomics focuses on the global exploration of endogenous small molecule metabolites as the end products of cellular processes in a biological system at the cell, tissue, organ or organism scale^{9, 10}. Therefore, metabolic profiling can provide a window into instantaneous and long-term physiological or pathological changes and thereby supplement the transcriptomic and proteomic profiling of the systematic and functional study of living organisms^{11, 12}. This method has been used successfully in identifying novel clinical biomarkers and therapeutic targets, especially in cancer.¹³ Recent reports have implicated the importance of metabolomics in the possible identification of biomarkers.¹⁴ To gain better insight into AS metabolism and to identify biomarkers with potential diagnostic value for predicting AS, a sensitive ultra-performance liquid chromatography coupled with quadruple time-of-flight mass spectrometry (UPLC Q-TOF/MS) method was developed for the analysis of endogenous metabolites in chicken livers. Thus, the goal of the present study was to use multivariate statistical data reduction tools to identify the low-molecular-weight metabolites and pathways of low-temperature-induced AS in broilers, an important area for future therapeutic intervention in metabolic diseases.

Methods

Experimental Design and Animal Management

Two hundred sixteen day-old male broilers (Ross-308) were randomly divided into two groups (control and model groups), each with six replicates of 18 broilers purchased from a local broiler breeder and hatchery farm, Zhengda Broiler Development Center of China Agriculture University in Hebei, China. Each replicate, which had an initial average body weight of 47.74 ± 0.55 g, was reared in a single cage ($2.4 \times 0.6 \times 0.6$ m) with a wire screen floor. The broilers had free access to water and feed and 23 h of illumination per day throughout the trial. The broilers' diet, which was in pellet form, was formulated to meet or exceed all nutrient requirements (NRC, 1994).¹⁵ The temperature in the broiler house during the first week was 32 to 35°C; it was then lowered by 1°C every other day until it reached 27°C. The method of inducing AS through

exposure to low temperatures was based on previous studies^{16,17,18}: starting on day 14, birds from the AS model group were exposed to a temperature cycle of 17°C during the daytime and 14°C at night until the end of the experiment to increase AS susceptibility, while birds from the control group were still exposed to a temperature of 27°C. The study was conducted in accordance with the Regulations of Experimental Animal Administration issued by the State Committee of Science and Technology of the People's Republic of China. The animal use protocol was approved by the Animal Care and Use Committee of the Poultry Institute at the Chinese Academy of Agriculture Science.

Sample Collection

At days 21 and 35, prior to the syndrome peak at 39 days,¹⁹ three birds were selected from each replicate (18 birds from each group) and weighed after 8 h of feed deprivation. Before the necropsy, 1.5 ml blood samples were collected from a wing vein into EDTA-K3 anticoagulation tubes to measure hematocrit (HCT) (Sysmex KX-21N Automatic blood analyzer, Kobe, Japan), and 1.5 ml of blood was centrifuged at 3500 g for 10 min so that serum could be collected for clinical blood chemistry detection.

The birds were then killed by jugular bleeding, and the hearts were removed and dissected. The weights of the right ventricle and the entire ventricle were recorded to calculate the heart index (HI) and the ascites heart index (AHI).²⁰ The lungs were removed and placed into a 10% formaldehyde solution. After being weighed for the liver index (LI) calculation, the livers were immediately washed with physiological saline, minced and homogenized with physiological saline (2-fold volume), and then stored at -80°C until analysis. Based on the results of these analyses, 6 birds from the AS group were determined to be AS birds. The criteria for this selection were based on the following three aspects: (1) $HCT \geq 0.36$; (2) $AHI \geq 0.28$; and (3) yellow liquid in abdominal cavity and pericardium^{21,22}. The liver tissues of 6 healthy birds from the control group and 6 AS birds from the model group were selected for metabolomic profiling.

Clinical blood chemistry determination

Low density lipoprotein cholesterol (LDLC) and cholesterol and total protein (TP) were determined

using a Unicel DXC 800 (Beckman Coulter, Fullerton, CA).

Histopathology Examination

To investigate the histopathological changes in the pulmonary artery associated with AS, segments with a thickness of 0.5 cm adjacent to the bronchi were removed from the lungs (6 from each group) and placed into a 10% formaldehyde solution for more than 24 h. They were then dehydrated in an ascending gradient of ethanol. After becoming transparent in dimethylbenzene, the lung tissues were embedded in paraffin and routinely processed into sections of 5 μm in depth followed by Weigert–van Gieson staining for elastin.²³ Small pulmonary arterioles with an external diameter in the range from 20 to 50, 50 to 100 and 100 to 200 μm were studied using an automatic image analyzer (BH2, Olympus, Japan) and the Motic 3.0 software. Twelve average cross-sectional regions were chosen. The adventitia and the lumen diameters were measured, and the relative medial thickness (RMT, %) was recorded and analyzed. The relative medial thickness of pulmonary arterioles with different cut angles and either contracted or relaxed conditions was computed from the above measurements according to previously described methods.^{24,25}

Metabolomic Sample Preparations

Liver samples (100 μL) were thawed at 4 $^{\circ}\text{C}$ and vortexed for 5 min in 0.25 mL of acetonitrile, which had been refrigerated for 30 min at 4 $^{\circ}\text{C}$, in an ice bath. Following centrifugation (12,000 rpm, 15 min, 4 $^{\circ}\text{C}$), 300 μL of supernatant was removed and then analyzed by UPLC. The sample order was randomized for analysis.

Chromatographic Separation

The UPLC analysis was performed with a Waters Acquity Ultra Performance LC system (Waters, Milford, MA) equipped with a Waters SYNAPT G2 Q-TOF HDMS (Waters MS Technologies, Manchester, UK). Chromatographic separation was conducted at 45 $^{\circ}\text{C}$ on an ACQUITY UPLC BEH C₁₈ column (2.1 mm \times 100 mm, 1.7 μm , UK). The mobile phase consisted of water (A) and acetonitrile (B), each containing 0.1% formic acid. The optimized UPLC elution conditions for liver samples were as follows: 0–0.5 min, 1%B; 0.5–2.0 min, 1–50% B; 2.0–9.0 min, 50–99% B, 9.0–10.0 min, 99% B and 10.0–12.0 min, 99–1% B. The flow

rate was 0.45 mL/min. The autosampler was maintained at 4 $^{\circ}\text{C}$. One microliter of sample solution was injected for each run.

Mass Spectrometry

Mass spectrometry was performed on a SYNAPT G2 Q-TOF HDMS (Waters MS Technologies, Manchester, UK), a quadruple and orthogonal acceleration time-of-flight tandem mass spectrometer. The scan range was from 50 to 1200 m/z. For the positive electrospray mode, the capillary and cone voltages were set at 3.2 kV and 45 V, respectively. For the negative electrospray mode, the capillary and cone voltages were set at 3.0 kV and 40 V, respectively. The desolvation gas was set to 800 L/h at a temperature of 450 $^{\circ}\text{C}$; the cone gas was set to 50 L/h; and the source temperature was set to 120 $^{\circ}\text{C}$. The mass spectrometer was operated at 25000 resolution using dynamic range extension. The data acquisition rate was set to 0.2 s. All analyses were acquired using the lockspray to ensure accuracy and reproducibility.

Leucine–enkephalin ($[\text{M}+\text{H}]^+=556.2771$, $[\text{M}-\text{H}]^+=554.2615$) was used as the lockmass at a concentration of 200 ng/mL and a flow rate of 5 $\mu\text{L}/\text{min}$. Data were collected in continuum mode. The lockspray frequency was set at 10 s, and data were averaged over 10 scans. All the data acquisition and analysis steps were controlled by the Waters MassLynx v4.1 software.

Data Analysis

The mass data were imported to Markerlynx XS (Waters Corporation, Milford, MA) within the Masslynx software for peak detection and alignment. All data were normalized to the summed total ion intensity per chromatogram, and the resultant data matrices were imported into the EZinfo 2.0 software (Waters Corporation, Milford, MA) for Principle Component Analysis (PCA) and Orthogonal Partial Least Squares Discriminant Analysis (OPLS-DA). Metabolite peaks were assigned by MS^E analysis or interpreted with available biochemical databases, such as HMDB (<http://www.hmdb.ca/>), Chemspider (<http://www.chemspider.com/>) and KEGG (<http://www.kegg.com/>). Potential markers were extracted from S plots constructed from analyses with OPLS-DA, and the markers were chosen based on their contribution to the variation and correlation within the data set. The reconstruction pathway analysis was performed with the MetPA software

(<http://metpa.metabolomics.ca>) based on the above data to identify the metabolic pathways.²⁶ Other statistical analyses were performed using SPSS 11.0 (SPSS Inc., Chicago, IL). Differences were considered significant when test *p* values were less than 0.05.

Results

Physical and biochemical parameters

Figure 1 shows the physical performance parameters of the control and model groups at 21 and 35 days. Body weights were markedly lower in the low-temperature-induced AS group compared with those in the control group, and all relationships were statistically significant ($p < 0.01$) at the two time points. Organ index values for the heart and liver and ascites heart index (AHI) values were all significantly increased in the AS group compared to the control group ($p < 0.01$). Figure 2 shows the comparisons of related biochemical parameters in blood between the control and model groups at 21 and 35 days. The HCT values were remarkably higher in the AS model group than in the control group at 21 and 35 days ($p < 0.01$). The TP, LDLC and cholesterol level values were significantly up-regulated in the model group at 21 days, and the TP and LDLC values continually increased to 35 days. The other parameters showed no significant statistical changes (data not shown).

Histological results

The external diameters of the pulmonary arteries were similar between the two groups, being within either $20 \leq R \leq 50$, $50 \leq R \leq 100$ or $100 \leq R \leq 200$ μm at different time points, while the RMT values were significantly different between the groups. The results are shown in Figure 3. The RMT values from different external diameters were all significantly higher in the AS model group than in the control group at 21 and 35 days. Figure 4 illustrates the histological findings of pulmonary arteriole remodeling with external diameters ranging from 20 to 50 μm between the two groups at 35 days.

Validation of UPLC-MS Conditions

The precision and the repeatability of the UPLC-MS method were validated by the reduplicate analysis of six injections of same quality control samples and six parallel samples prepared

using the same preparation method, respectively. The relative standard deviation (RSD) of retention time and peak area are below 0.82% and 3.4%. The resulting data showed that the precision and repeatability of the proposed method were satisfactory for metabolomic analysis.

Metabolomics Profiling and Pattern recognition analysis

Liver samples were measured both in the positive and negative ion mode. We observed higher noise and matrix effects in the positive ion mode, resulting in a higher baseline and the subsequent omission of certain metabolites of low abundance and the concomitance of multiple adduction ions. To maximize metabolite detection and data quality, the negative ion mode was applied in the final analysis.

Metabolic profiling of liver samples was acquired using UPLC Q-TOF/MS in the negative ion mode. The base peak intensity (BPI) chromatograms of liver samples at 21 and 35 days from the control and model groups are shown in Figure 5. OPLS-DA was used for multivariate projection because its ability to identify discriminatory variables is based on an analysis of the OPLS weights. According to the UPLC-MS data, 5217 negative ion peaks were detected and processed by MarkerLynx XS using the same acquisition method. The metabolic liver patterns for broilers from each group at 21 (Figure 6A) and 35 (Figure 6B) days were plotted using OPLS-DA in the negative ion mode. Based on the OPLS-DA analysis, the control and low-temperature-induced groups were significantly divided into two clusters. Combined with previous data, this result suggested that an AS model was successfully reproduced in the negative ion mode and that members of the AS group had significantly different liver metabolisms, which resulted in a significant increase in the liver index values during clinical diagnosis. Hence the altered profiling of liver metabolites at 21 and 35 days could reflect changes in liver metabolism caused by AS.

Identification and comparisons of potential biomarkers

The S-plots of liver tissue samples at 21 and 35 days that were used to find potential biomarkers are shown in Figure 7A and 7B, respectively. The ions farthest from the origin contribute significantly to the separation of the two groups and may be

regarded as the potential biomarkers for low-temperature-induced ascites syndrome. The potential biomarkers were predicted by comparing accurate MS data with the metabolites and searching in Chemspider, HMDB and KEGG. According to the possible fragment mechanisms, compounds without information related to a given mass fragment were removed from the candidate list and only the most probable compounds were reserved^{27,28,29}. An *m/z* value of 188.07 is shown here as an example to illustrate the identification process. In addition to the base peak ion at *m/z* 188.0715, the ion at *m/z* 205.09 was found in positive ion spectrum (Figure 8A). Thus, we infer that the quasi-molecular ion is *m/z* 205.09 ($[M+H]^+$), and the ion at *m/z* 188.0715 is the fragment ion ($[M+H-NH_3]^+$). The base peak ion is *m/z* 203.08 ($[M-H]^-$) in the negative ion spectrum (Figure 8C). Therefore, the quasi-molecular ions were found to be *m/z* 205.09 ($[M+H]^+$) in ESI⁺ and *m/z* 203.08 ($[M-H]^-$) in ESI⁻. The fragment ions at *m/z* 146.06 and *m/z* 118.06 are $[M^+H-NH^3-C_2H_2O]^+$ and $[M^+H-NH^3-C_2H_2O-CO]^+$ in the product ion scan spectrum, respectively (Figure 8B).^{30,31} Accordingly, the molecule was identified as tryptophan. By comparing the retention times and mass spectra to the authentic chemicals, a portion of the low-temperature-related metabolites were structurally confirmed. The identified biomarkers are summarized in Tables 1 and 2.

To investigate the changes of the potential biomarkers in the livers of the AS model chickens, we compared the relative intensity of putative potential biomarkers between the control and model groups at 21 and 35 days (Figure 9A and 9B). At 21 days, the concentrations of cholic acid glucuronide, prostaglandin E2 glyceryl ester (PGE2-G), leukotriene B4 dimethylamide, leukotriene E3, prostaglandins, lysoPC(15:0), sphingosine 1-phosphate, sodium taurocholate and taurine were all up-regulated compared to the control group, while the concentrations of taurodeoxycholic acid, glycocholic acid, leukotriene E4, taurocholic acid and ursodeoxycholic acid were down-regulated. At 35 days, the concentrations of taurocholic acid, cholic acid glucuronide and sphingosine 1-phosphate were up-regulated, while the concentrations of taurodeoxycholic acid, lysoPE(18:0/0:0), glycocholic acid, lysoPC(17:0), myoinositol, lysoPC(18:0), lysoPC(15:0), lysoPC(16:0), tryptophan, lysoPE(22:4(7Z,10Z,13Z,16Z)/0:0) and

lysoPE(20:2(11Z,14Z)/0:0) were all down-regulated compared to the control group.

In addition, OPLS-DA loading plots were generated at 21 (Figure 10A) and 35 (Figure 10B) days. The loading plots indicated which metabolites were quantitatively higher or lower in the AS model group compared to the control group. The coefficients of the metabolites help to validate the accuracy of the altered trend shown in Figure 9. The altered trends of different biomarkers are also summarized in Table 1 and Table 2.

The acquired data were analyzed using MetaboAnalyst's data annotation tools to further investigate the AS-related profiles. The correlation analysis plot of differential metabolites (Figure 11) and the heatmap visualization (Figure 12) for the AS group at 21 and 35 days were all distinctly segregated. These models were capable of distinguishing AS chickens by adjusting multiple metabolic pathways from control subjects. From the plots, various metabolites could be identified as responsible for the separation between the model and control groups, and these were therefore viewed as potential biomarkers.

Metabolic Pathway and Functional Analysis

More detailed analyses of the pathways and networks influenced by low-temperature-induced AS were performed using MetPA, which is a free web-based tool that combines results from powerful pathway enrichment analysis with topology analysis. Metabolic pathway analysis with MetPA revealed that the metabolites that were identified together were important for the host response to AS. The results showed that at 21 days, the responsible pathways were taurine and hypotaurine metabolism, starch and sucrose metabolism, pentose and glucuronate interconversions, sphingolipid metabolism and glycerophospholipid metabolism. At 35 days, the different expressed pathways were starch and sucrose metabolism, pentose and glucuronate interconversions, sphingolipid metabolism, galactose metabolism, inositol phosphate metabolism, glycerophospholipid metabolism, tryptophan metabolism, and aminoacyl-tRNA biosynthesis. Most of these pathways were related to glucose and energy metabolism and lipid metabolism. Potential biomarkers were also identified from these relevant pathways. Some significantly changed metabolites were identified, and these were used to explain the

primary bile acids metabolism. These results suggest that these pathways show marked perturbations over the entire course of AS and could contribute to the development of AS.

Discussion

To our knowledge, this is the first study to systematically identify differently expressed metabolites in AS. To adequately reproduce the AS model, we referred to methods that had successfully replicated the disease. Meanwhile, we monitored the typical pathological features associated with AS.

Low temperatures require animals with higher metabolic burdens to maintain their body temperatures, resulting in metabolic hypoxia or low oxygen utilization efficiency.³² The central etiology of the disease is a hypoxemic condition resulting from an imbalance between oxygen requirements and oxygen supply. A cascade of compensatory mechanisms eventually leads to increased pulmonary pressure, which is initially overcome by right ventricular hypertrophy. If persistent, this leads to right ventricular valve insufficiency, volume overload, right heart dilatation, and right ventricular failure. At 21 and 35 days, the results showed that broilers in the model group had significantly higher HCT and AHI values, which were regarded as a threshold indicator of ascites and pulmonary hypertension.³³ The compensatory hyperplasia of the key organs resulted in a significant increase in the heart and liver index values in the model group compared with the control. In the histopathology examination, pulmonary artery remodeling was confirmed by the statistical analysis of RMT from different external diameters and microphotographs of pulmonary artery structures of the broilers' lungs, which were also regarded as typical parameters in the ascites syndrome.³⁴ These related remodeling pathways resulted in a bodyweight decrease at a significant level. In the metabolomic pattern analysis, two groups were clearly separated at 21 and 35 days. Thus, it is suggested that an AS model was successfully reproduced. Meanwhile, metabolomic profiling at different times resulted in a dynamic illustration of the pathological process.

By 21 days, several of the metabolites had been altered in response to low temperatures, and most were related to bile acids (BAs) metabolism. Liver disease results in profound changes in the patterns

of bile acids metabolism, some of which could be harmful and some of which could be protective.³⁵ BAs are steroid carboxylic acids derived from cholesterol in the livers of vertebrates. In the synthesis of primary hepatic BAs, the conjugation of free BAs with taurine or glycine appears to be a prerequisite for the efficient secretion of common BAs into bile.³⁶ The biomarkers detected in our study at 21 days showed that concentrations of conjugated BAs, such as taurodeoxycholic acid, glycocholic acid, and ursodeoxycholic acid, were significantly decreased in the model group, while the concentration of taurine showed a significant increase. Primary BAs synthesis was disrupted in the initial stages of AS. Meanwhile, the significantly increased level of the cholic acid glucuronide showed that the conjugation of this molecule with free BAs was up-regulated. Previous studies have reported that this formation appears to be a quantitatively minor pathway in bile acids metabolism.³⁷ However, increased concentrations of glucuronidated BAs have been found in humans with cholestatic liver diseases.³⁸ It was concluded that in the chickens' livers, AS interfered with the normal conjugation of free BAs and led to cholestasis. The glucuronidation of BAs is an important pathway for the detoxification and elimination of retained free BAs.³⁹ Another important metabolic pathway influenced by AS was arachidonic acid metabolism, which is the basic metabolism that produces prostaglandin and leukotrienes (LETs). Previous studies have reported that endogenous PG production in hepatocytes may regulate the secretion of BAs and play a protective role in the initial stages of cellular damage in rats.⁴⁰ Based on the significantly increased level of PGE2 glyceryl ester (PGE2-G) and prostaglandins at 21 days, we concluded that the liver may elicit a negative feedback to cholestasis. Further, LETs disorder at 21 days indicated an inflammatory response in the livers of chickens with ascites. These results suggested that the livers of chickens with ascites exhibited substantial problems in primary BAs synthesis and the inflammatory response, which was also a protective response mechanism in the initial stages.

At 35 days, most of the biomarkers were different from those observed at 21 days. The presence of primary BAs continued to disrupt conjugated BAs. Taurodeoxycholic acid, glycocholic acid and cholic acid glucuronide showed the same trends as those observed at 21 days. We can conclude that in the

later stages of AS, persistent primary BAs disrupt synthesis, resulting in lipid metabolism disorders in the liver. Most of the biomarkers detected at 35 days were lysophospholipids, which were related to phospholipid metabolism. Lysophospholipids play a crucial role in phospholipid metabolism and cell physiology, particularly as the product of phospholipase A activity both within and outside cells. Lipid peroxidation within cell membranes caused by reactive oxygen species is believed to play a significant role in the etiology of AS.⁴¹ When oxidative stress occurs, the generation of free radicals can activate the phospholipase A2, which could influence the production of lysophosphatidylcholine.⁴² The collective decline of lysophospholipids in the liver resulted in an increase of concentrations in the serum metabolomic profile (data not shown). Primary BAs metabolism and phospholipid metabolism in the model group were significantly different from those in the control at 35 days, which resulted in a significant disruption in lipid metabolism. Previous studies have suggested that myoinositol in rat livers helps to promote the transfer of fat into blood and protects the liver from lipid metabolism dysfunctions.⁴³ However, all of the related metabolites were significantly decreased in chickens with ascites, showing that lipid metabolism in the liver was markedly disrupted. Additionally, we found that the low temperatures significantly changed the serum concentrations of LDL-C, cholesterol and TP at 21 and 35 days. The changes in the concentrations of serum lipid and related metabolites at 21 and 35 days further support the notion that lipid metabolism and its related pathways play an important role in the pathological process of ascites in liver metabolism.

The comparisons of different metabolites at 21 and 35 days illustrate that the main pathways occurred at the beginning and at the peak of AS. According to the MetPA analysis data, several metabolic pathways appeared at both 21 and 35 days, while primary BAs metabolism was the most significant at both 21 and 35 days of AS. Most of the others related to glucose metabolism. In the identification and comparison of potential biomarkers, five metabolites, including taurodeoxycholic acid, cholic acid glucuronide, glycocholic acid, LysoPC(15:0) and taurocholic acid, were present at both 21 and 35 days in chickens with ascites, and these molecules were considered to be biomarkers throughout the process

in ascites chickens. Previous studies have always chosen one time point to screen biomarkers, while some potential biomarkers are not significant at two points. Biomarkers are indicators of biological processes and pathological states that can reveal a variety of healthy and disease traits.⁴⁴ They indicate the presence or extent of a biological process that is directly linked to the clinical manifestations and outcomes of a particular disease.⁴⁵ System analyses of metabolic networks, a central paradigm in biology, can help us identify new drug targets, which in turn, will generate a more in-depth understanding of the AS mechanism and thus provide better guidance at the level of global metabolomics.

Conclusions

In conclusion, the results of this study indicate that primary bile acids synthesis disorder and inflammation occurred at 21 days and that lysophospholipid metabolism was disrupted at 35 days after the continuation of low temperatures. Five metabolites, including taurodeoxycholic acid, cholic acid glucuronide, glycocholic acid, LysoPC(15:0) and taurocholic acid, were considered to be the most appropriate biomarkers for any stage of the disease. In future work, these potential biomarkers will be further validated with a larger cohort. The results help to identify potential mechanisms responsible for AS and provide possible biomarkers for this metabolic disease in poultry. While we consider this study a discovery project to validate the experimental paradigm and to elucidate pleiotropic features, the sample size is commensurate with other metabolomics studies. The findings indicate that a metabolomic-based approach was useful to comprehensively investigate the pathological process of a metabolic disease and this approach could be useful in the future.

Abbreviations used

AS	ascites syndrome
AHI	ascites heart index
BPI	base peak intensity
BAs	bile acids
HCT	hematocrit
HI	heart index
LI	liver index
LDL-C	low density lipoprotein cholesterol

OPLS-DA	orthogonal partial least squares discriminant analysis
PCA	principle component analysis
PGE2-G	prostaglandin E2 glyceryl ester
RMT	relative medial thickness
RSD	relative standard deviation
t _R	retention time
UPLC/Q-TOF/MS	ultra-performance liquid chromatography/quadruple time-of-flight mass spectrometry

Acknowledgments

We acknowledge the financial supports from the National Scientific Foundation Council of China (Nos. 31301994), Natural Science Foundation of Jiangsu (Nos. BK2012689), Chinese Universities Scientific Fund, China Agricultural Research System.

Author contributions

Y.S and S.S performed all measurements and analyzed the data. H.T. helped develop the measurement setup. J.Z. supervised and provided continuous guidance for the experiments and the analysis. Y.G. provided valuable theoretical guidance and insight. All authors discussed the results and contributed to manuscript revision.

These authors contributed equally to this work.
Yiru Shen & Shourong Shi

Competing financial interests

The authors declare no competing financial interests.

References

- Ginés, P., Quintero, E., Arroyo, V., Terés, J., Bruguera, M., Rimola, A. & Rozman, C. *Hepatology*, 1987, **7**, 122-128.
- D'amico, G., Morabito, A., Pagliaro, L., & Marubini, E. *Digestive diseases and sciences*, 1986, **31**, 468-475.
- Baghbanzadeh, A., & Decuypere, E. *Avian Pathology*, 2008, **37**, 117-126.
- Haslam, S. M., Knowles, T. G., Brown, S. N., Wilkins, L. J., Kestin, S. C., Warriss, P. D., & Nicol, C. *British Poultry Science*, 2008, **49**, 685-696.
- Aksit, M., Altan, O., Karul, A. B., Balkaya, M., & Ozdemir, D. *Archiv fur Geflugelkunde*, 2008, **72**, 221-230.
- Kalmar, I. D., Vanrompay, D., & Janssens, G. P. *The Veterinary Journal*, 2013, **197**, 169-174.
- Hutchison, T. W., & Riddell, C. *The Canadian Veterinary Journal*, 1990, **31**, 20.
- Julian, R. J. *Avian pathology*, 1993, **22**, 419-454.
- Nicholson JK, Lindon JC. *Nature*, 2008, **455**, 1054-1056.
- Zhang AH, Sun H, Wang XJ. *Anal Bioanal Chem*, 2013, 1-8.
- Johnson CH, Gonzalez FJ. *J Cell Physiol*, 2012, **227**, 2975-2981.
- Mamas M, Dunn WB, Neyses L, Goodacre R. *Arch Toxicol*, 2011, **85**, 5-17.
- Sreekumar, A., Poisson, L. M., Rajendiran, T. M., Khan, A. P., Cao, Q., Yu, J. & Chinnaiyan, A. M. *Nature*, 2009, **457**, 910-914.
- Mangalam, A. K., Poisson, L. M., Nemutlu, E., Datta, I., Denic, A., Dzeja, P. & Giri, S. *Journal of clinical & cellular immunology*, 2013, **4**.
- NRC. 1994. *Nutrient Requirements of Poultry*. 9th rev. ed. National Academies Press, Washington, DC.
- Geng, A., Li, B., & Guo, Y. *Archives of Animal Nutrition*, 2007, **61**, 50-60.
- Wang, Y., Guo, Y., Ning, D., Peng, Y., Cai, H., Tan, J. & Liu, D. *Journal of animal science and biotechnology*, 2012, **3**, 41.
- Yang, Y., Gao, M., Wu, Z., & Guo, Y. *European journal of pharmacology*, 2010, **649**, 242-248.
- Wideman, R. F., Rhoads, D. D., Erf, G. F., & Anthony, N. B. *Poultry science*, 2013, **92**, 64-83.
- Julian, R. J., Frazier, J. A., & Goryo, M. *Avian Pathology*, 1989, **18**, 161-173.
- Geng, A. L., Guo, Y. M., & Yang, Y. *Poultry science*, 2004, **83**, 1587-1593.
- Geng, A. L., & Guo, Y. M. *British poultry science*, 2005, **46**, 626-634.
- Herget, J. *Physiol. Res*, 1991, **40**, 129-137.
- Tan, X.; Liu, Y. J.; Li, J. C.; Pan, J. Q.; Sun, W. D.; Wang, X. L. *Res. Vet. Sci*, 2005, **79**, 131-137.
- Barth, P. J., Kimpel, C. H., Roy, S., & Wagner, U. *Pathology-Research and Practice*, 1993, **189**, 567-576.
- Xia J, Mandal R, Sinelnikov I V, et al. *Nucleic acids research*, 2012, **40**, W127-W133.
- Zhao, Y. Y., Cheng, X. L., Wei, F., Bai, X., Tan, X. J., Lin, R. C., & Mei, Q. *Journal of proteome research*, 2013, **12**, 692-703.
- Zhao, Y. Y., Cheng, X. L., Wei, F., Bai, X., & Lin, R. C. *Biomarkers*, 2012, **17**, 721-729.

- 29 Zhao, Y. Y., Zhang L, Long F. Y., Cheng, X. L., Bai, X, Wei, F. & Lin, R. C. *Chemico-Biological Interactions*, 2013,**301**,31–38.
- 30 Zhao, Y. Y., Liu, J., Cheng, X. L., Bai, X., & Lin, R. C. *ClinicaChimicaActa*, 2012, **413**, 642-649.
- 31 Zhao, Y. Y., Feng, Y. L., Bai, X., Tan, X. J., Lin, R. C., & Mei, Q. *PloS one*, 2013,**8**, e59617.
- 32 Julian, R.J., *Poultry Science*, 1998, **77**, 1773–1780.
- 33 Peng, Y. Z., Wang, Y. W., Ning, D., &Guo, Y. M. *Avian Pathology*, 2013 (just-accepted).
- 34 Yang, Y., Qiao, J., Wang, H., Gao, M., Ou, D., Zhang, J. &Guo, Y. *European journal of pharmacology*, 2007,**561**, 137-143.
- 35 Palmer, R. H. *Archives of internal medicine*, 1972,**130**, 606.
- 36 Lefebvre, P., Cariou, B., Lien, F., Kuipers, F., &Staels, B. *Physiological reviews*, 2009,**89**, 147-191.
- 37 Hofmann, Alan F. *Hepatology*, 2007,**45.4**, 1083-1084.
- 38 Stiehl, A., Raedsch, R., Rudolph, G., Gundert - Remy, U., &Senn, M. *Hepatology*, 1985, **5**, 492-495.
- 39 Danielsson, H., &Sjovall, J. *Annual review of biochemistry*, 1975, **44**, 233-253.
- 40 GUARNER, F., FREMONT. SMITH,M.A.U.R.I.C.E.,&PRIETO, J. *Liver*,1985,**5**, 35-39.
- 41 Bottje, W. G., &Wideman Jr, R. F. *Poultry and Avian Biology Reviews*, 1995,**6**.
- 42 Bassa, B. V., Noh, J. W., Ganji, S. H., Shin, M. K., Roh, D. D., &Kamanna, V. S. *Biochimica et BiophysicaActa (BBA)-Molecular and Cell Biology of Lipids*, 2007,**1771**, 1364-1371.
- 43 Burton, L. E., & Wells, W. W. *The Journal of nutrition*, 1976, **106**, 1617.
- 44 Kind, T., Tolstikov, V., Fiehn, O., & Weiss, R. H. *Analytical biochemistry*, 2007, **363**, 185-195.
- 45 Sun, H., Zhang, A., Yan, G., Piao, C., Li, W., Sun, C. & Wang, X. *Molecular & Cellular Proteomics*, 2013, **12**, 710-719

Table 1

14 biomarkers of ascites syndrome detected by UPLC Q-TOF/MS in negative ion mode (21days)

No	t_R (min)	Metabolite	m/z	Elemental composition	Quasi-molecular ion	Formula	Trend ^a	Related pathways
1	2.79	Taurodeoxycholic acid	498.2890	C ₂₆ H ₄₄ NO ₆ S	[M-H] ⁻	499.7040	↓***	BAs metabolism
2	4.45	Cholic acid glucuronide	619.2885	C ₃₀ H ₄₈ O ₁₁ Cl	[M+Cl] ⁻	584.6955	↑***	BAs metabolism
3	7.36	PGE2-G	485.2822	C ₂₅ H ₄₁ O ₉	[M+CH ₃ COO] ⁻	426.5436	↑***	Arachidonic acid metabolism
4	2.78	Glycocholic acid	500.2906	C ₂₆ H ₄₃ NO ₆ Cl	[M+Cl] ⁻	465.6227	↓***	BAs metabolism
5	2.79	Leukotriene E4	498.2118	C ₂₅ H ₄₀ NO ₇ S	[M+CH ₃ COO] ⁻	439.609	↓***	Arachidonic acid metabolism
6	5.89	Leukotriene B4 dimethylamide	362.2365	C ₂₂ H ₃₆ NO ₃	[M-H] ⁻	363.5341	↑***	Arachidonic acid metabolism
7	7.35	Leukotriene E3	486.2855	C ₂₄ H ₄₀ NO ₇ S	[M+HCOO] ⁻	441.6240	↑***	Arachidonic acid metabolism
8	5.25	Prostaglandins	387.2398	C ₂₀ H ₃₅ O ₇	[M-H] ⁻	388.4956	↑***	Arachidonic acid metabolism
9	6.24	LysoPC(15:0)	480.3092	C ₂₃ H ₄₇ NO ₇ P	[M-H] ⁻	481.6035	↑*	Phospholipid metabolism
10	5.35	Sphingosine 1-phosphate	410.2366	C ₁₈ H ₃₇ NO ₇ P	[M+CH ₃ COO] ⁻	351.4186	↑***	Phospholipid metabolism
11	4.41	Sodium taurocholate	596.2918	C ₂₄ H ₄₀ NO ₇ S	[M+HCOO] ⁻	441.624	↑***	BAs metabolism
12	2.54	Taurocholic acid	514.2839	C ₂₆ H ₄₄ NO ₇ S	[M-H] ⁻	515.703	↓	BAs metabolism
13	3.91	Ursodeoxycholic acid	391.2849	C ₂₄ H ₃₉ O ₄	[M-H] ⁻	392.572	↓***	BAs metabolism
14	0.54	Taurine	124.0076	C ₂ H ₆ NO ₃ S	[M-H] ⁻	125.147	↑***	BAs metabolism

^a Change trend of the model group vs the control group

The levels of potential biomarkers were labeled with (↓) down-regulated and (↑) up-regulated.

* $p < 0.05$, ** $p < 0.01$ and *** $p < 0.001$

Table 2

14 biomarkers of ascites syndrome detected by UPLC Q-TOF/MS in negative ion mode (35days)

No	t _R (min)	Metabolite	m/z	Elemental composition	Quasi-molecular ion	Formula	Trend ^b	Related pathway
1	2.54	Taurocholic acid	514.2839	C26H45NO7S	[M-H]-	515.703	↑**	Bas metabolism
2	2.79	Taurodeoxycholic acid	498.2890	C26H44NO6S	[M-H]-	499.7040	↓	Bas metabolism
3	5.11	LysoPE(18:0/0:0)	480.3090	C23H47NO7P	[M-H]-	481.6035	↓***	Phospholipid metabolism
4	4.45	Cholic acid glucuronide	619.2885	C30H48O11Cl	[M+Cl]-	584.6955	↑***	Bas metabolism
5	2.78	Glycocholic acid	500.2782	C26H43NO6 Cl	[M+Cl]-	465.6227	↓***	Bas metabolism
6	6.28	LysoPC(17:0)	508.3403	C25H51NO7P	[M-H]-	509.6566	↓***	Phospholipid metabolism
7	0.54	Myoinositol	215.0322	C6H12O6 Cl	[M+Cl]-	180.1559	↓***	
8	6.283	LysoPC(18:0)	568.3613	C27H55NO9P	[M+HCOO]-	523.6832	↓***	Phospholipid metabolism
9	6.24	LysoPC(15:0)	480.3092	C23H47NO7P	[M-H]-	481.6035	↓***	Phospholipid metabolism
10	5.11	LysoPC(16:0)	540.3301	C24H49NO7P	[M+HCOO]-	495.6301	↓***	Phospholipid metabolism
11	1.73	Tryptophan	203.0820	C11H12N2O2	[M-H]-	204.2252	↓***	
12	7.25	Sphinganine 1-phosphate	426.3001	C18H40NO5P	[M+HCOO]-	381.4877	↑***	Lipid metabolism
13	4.51	LysoPE(22:4(7Z,10Z,13Z,16Z)/0:0)	528.3091	C27H48NO7P	[M-H]-	529.6463	↓***	Phospholipid metabolism
14	4.48	LysoPE(20:2(11Z,14Z)/0:0)	504.3090	C25H47NO7P	[M-H]-	505.6249	↓***	Phospholipid metabolism

^a Change trend of the model group vs the control group

The levels of potential biomarkers were labeled with (↓) down-regulated and (↑) up-regulated.

p*<0.05, *p*<0.01 and ****p*<0.001

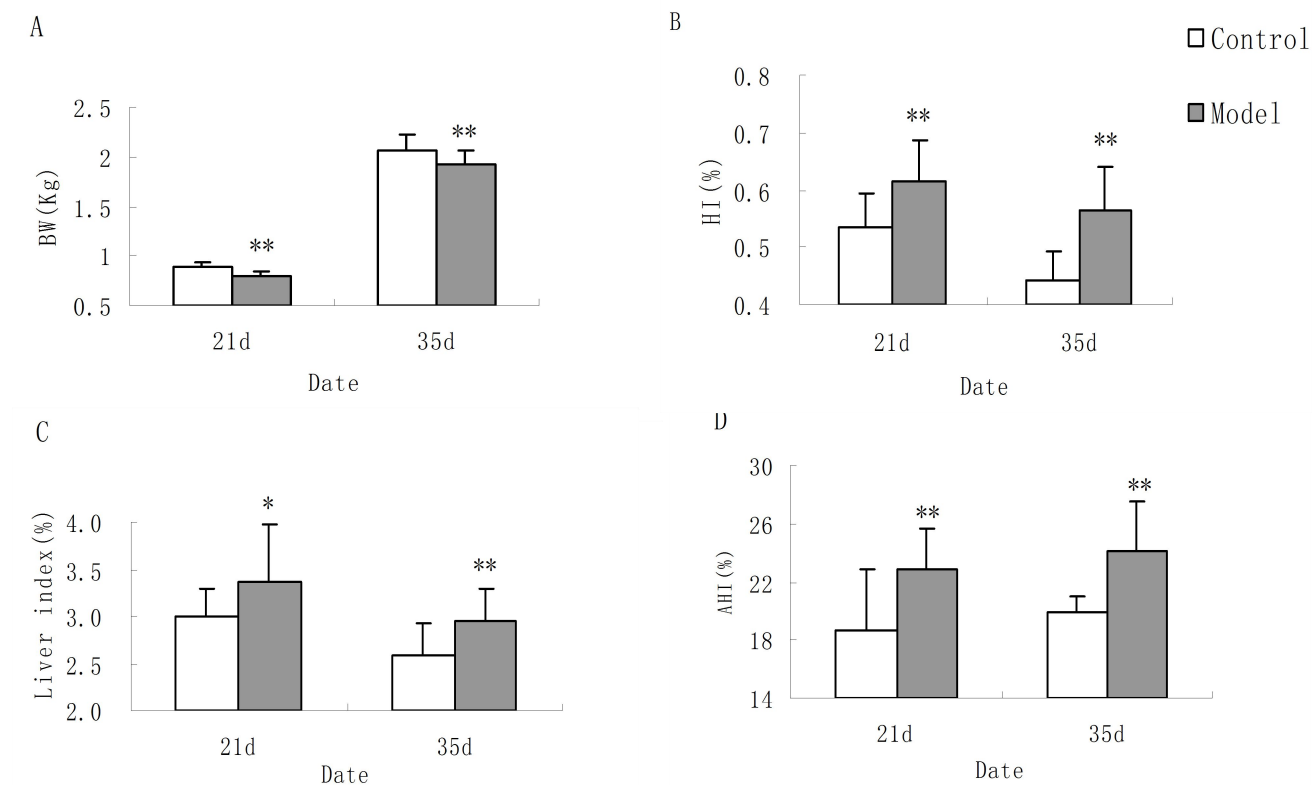


Figure 1. Physical parameter comparisons between the AS and control groups. (A) Body weight; (B) Heart index; (C) Liver index; (D) Ascites heart index. The data were expressed as the mean \pm SD
**significant difference compared with control groups ($P < 0.01$)

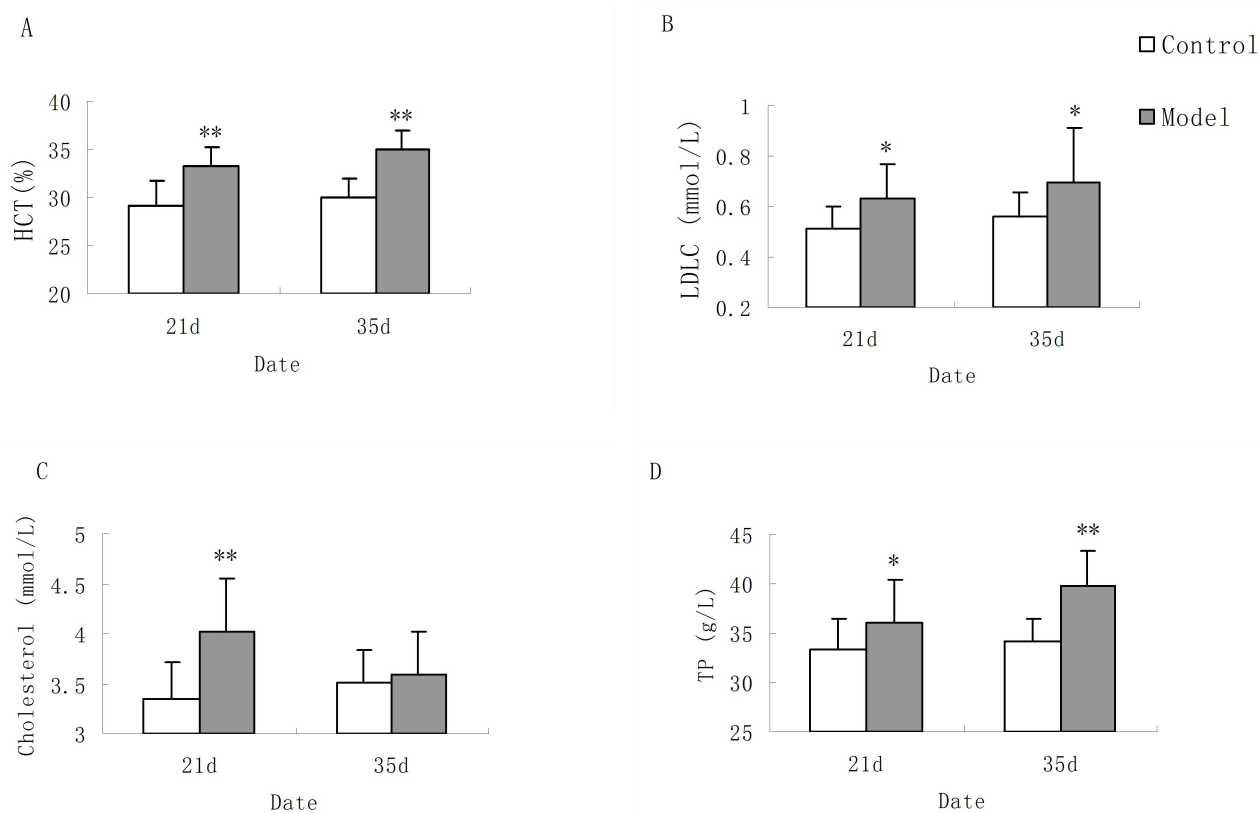


Figure 2. Blood parameter comparisons between the AS and control groups. (A) Hematocrit (HCT); (B) Low density lipoprotein cholesterol (LDLC); (C) Cholesterol; (D) Total protein (TP). The data were expressed as the mean \pm SD **significant difference compared with control groups ($P < 0.01$) * significant difference compared with control groups ($P < 0.05$)

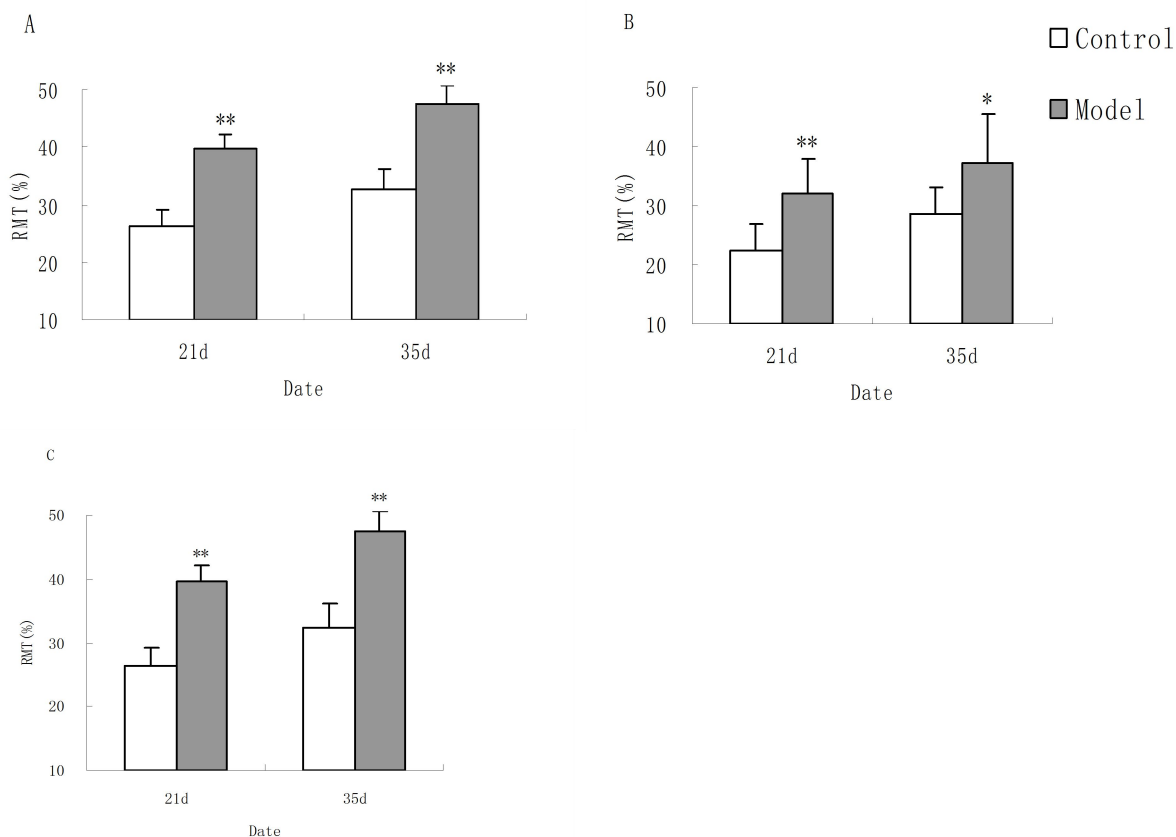


Figure 3. Relative medial thickness (RMT) of pulmonary arteriole with external diameters ranging from 20 to 50, 50 to 100 μm and 100 to 200 μm in the AS and control groups. (A) 20-50 μm ; (B) 50-100 μm ; (C) 100-200 μm . The data were expressed as the mean \pm SD **significant difference compared with control groups ($P < 0.01$). *significant difference compared with control groups ($P < 0.05$).

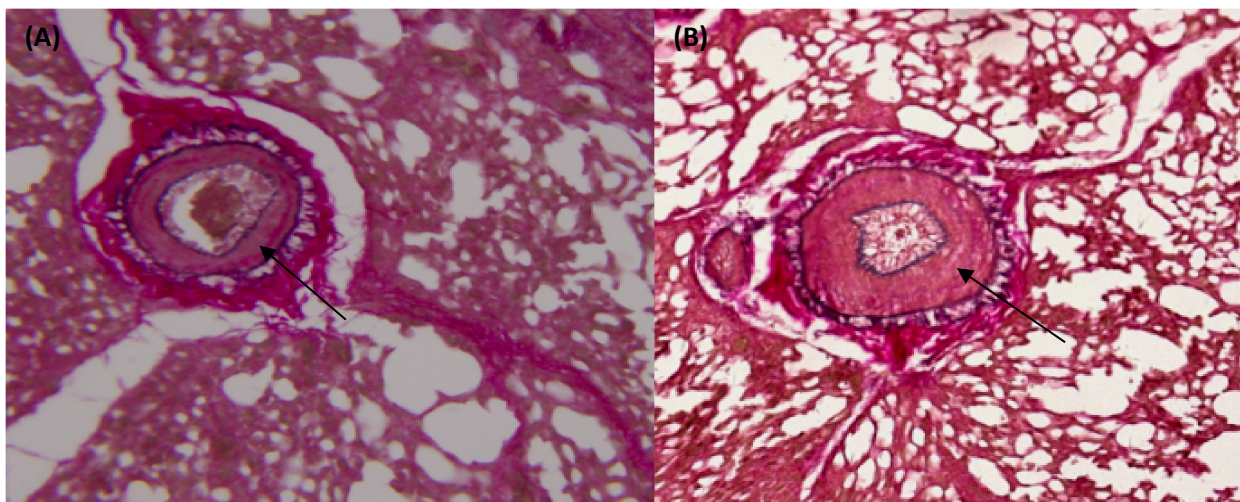


Figure 4. Histological change of pulmonary arteriole structure with pulmonary arteriole external diameter ranging from 20 to 50 μm (Weigert-Van Gieson $\times 100$) in the (A) control and (B) AS birds.

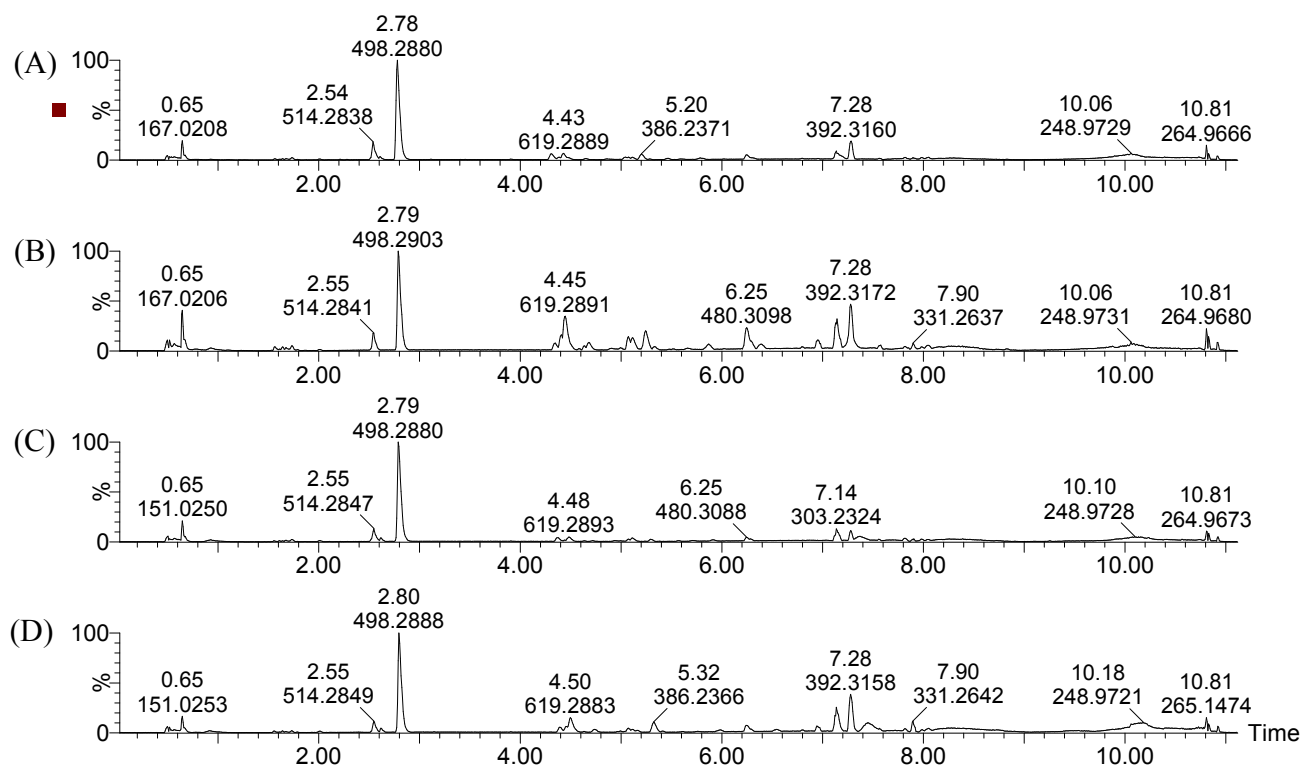


Figure 5. Base peak intensity (BPI) chromatograms obtained from liver samples from the control group (A) and the model group (B) on the 21st day and the control group (C) and the model group (D) on the 35th day.

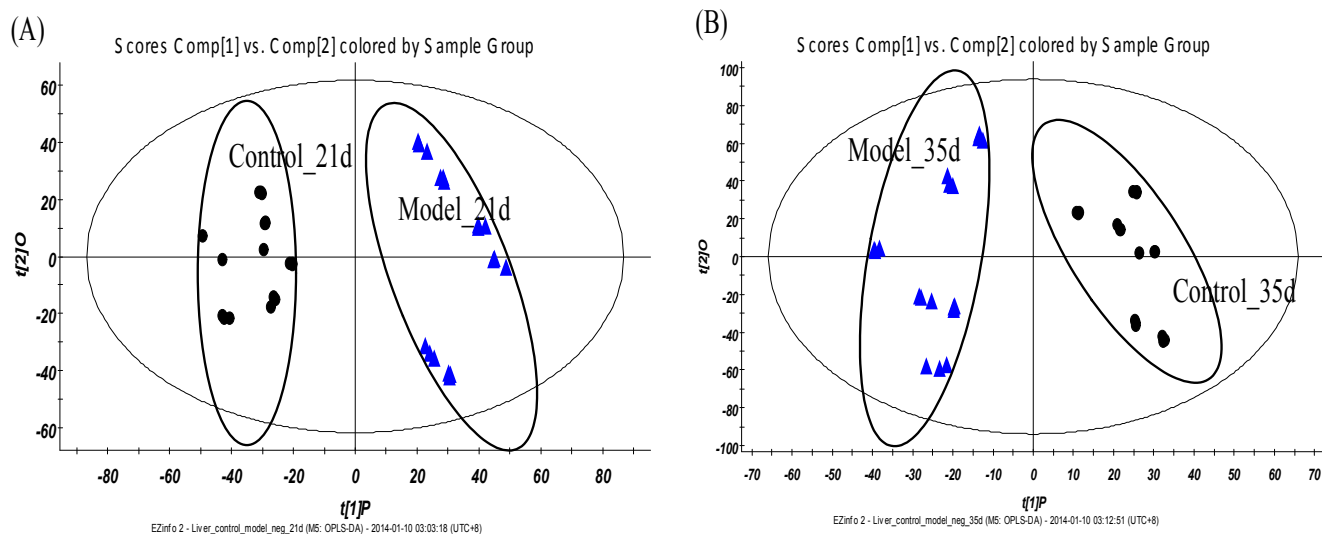


Figure 6. The OPLS-DA score plots derived from the UPLC-MS profiles of liver samples from the control group and the model group on the 21st day (A) and the 35th day (B).

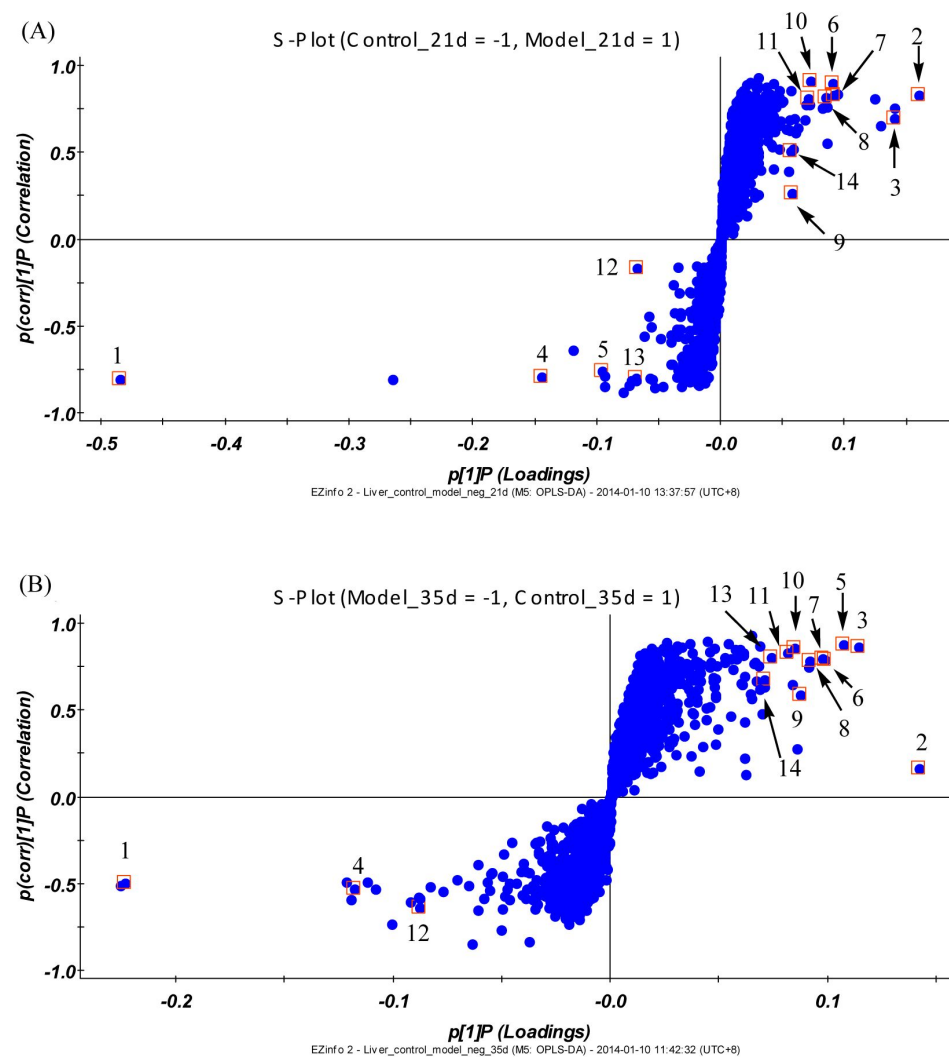


Figure 7. S-plot used in biomarker selection at the 21st day (A) and the 35th day (B). The variables marked (\square) are the metabolites selected as potential biomarkers. The variables far from the origin contributed significantly to differentiate the clustering of the model group from that of the normal control group and were considered as potential biomarkers.

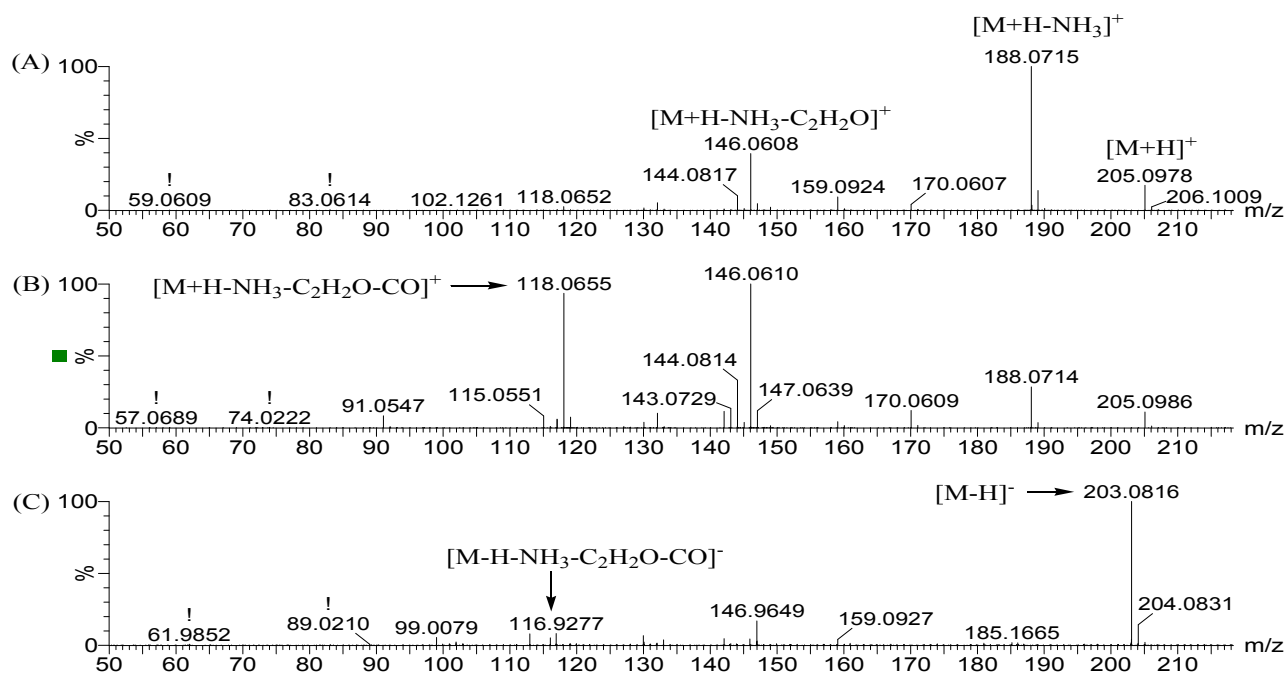


Figure 8. Mass spectra of biomarker at (A) m/z 188.07 in positive ion mode, (B) product ion scan spectrum of the biomarker in positive ion mode, (C) m/z 203.08 in negative ionization mode.

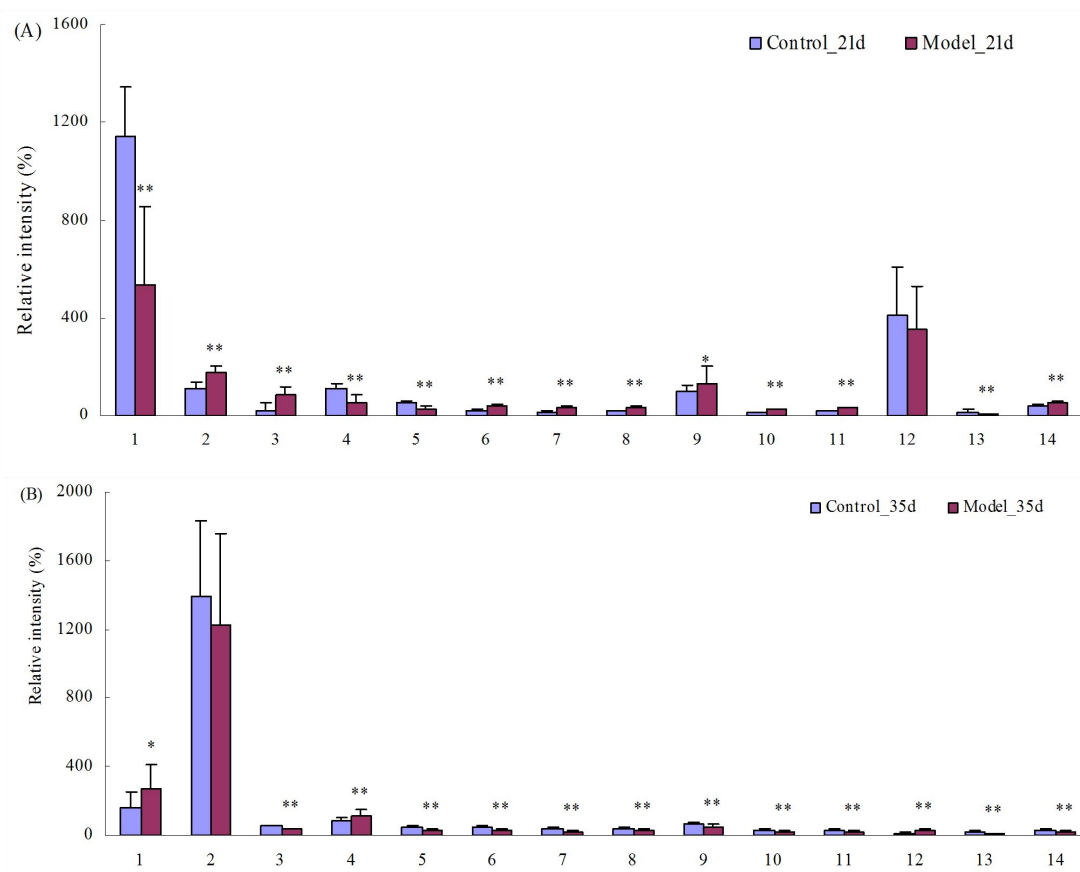


Figure 9. Comparison of the relative intensity of putative potential biomarkers in the normal control and model groups on the 21st day (A) and 35th day (B). The numbers correspond with Tables 1 and 2.

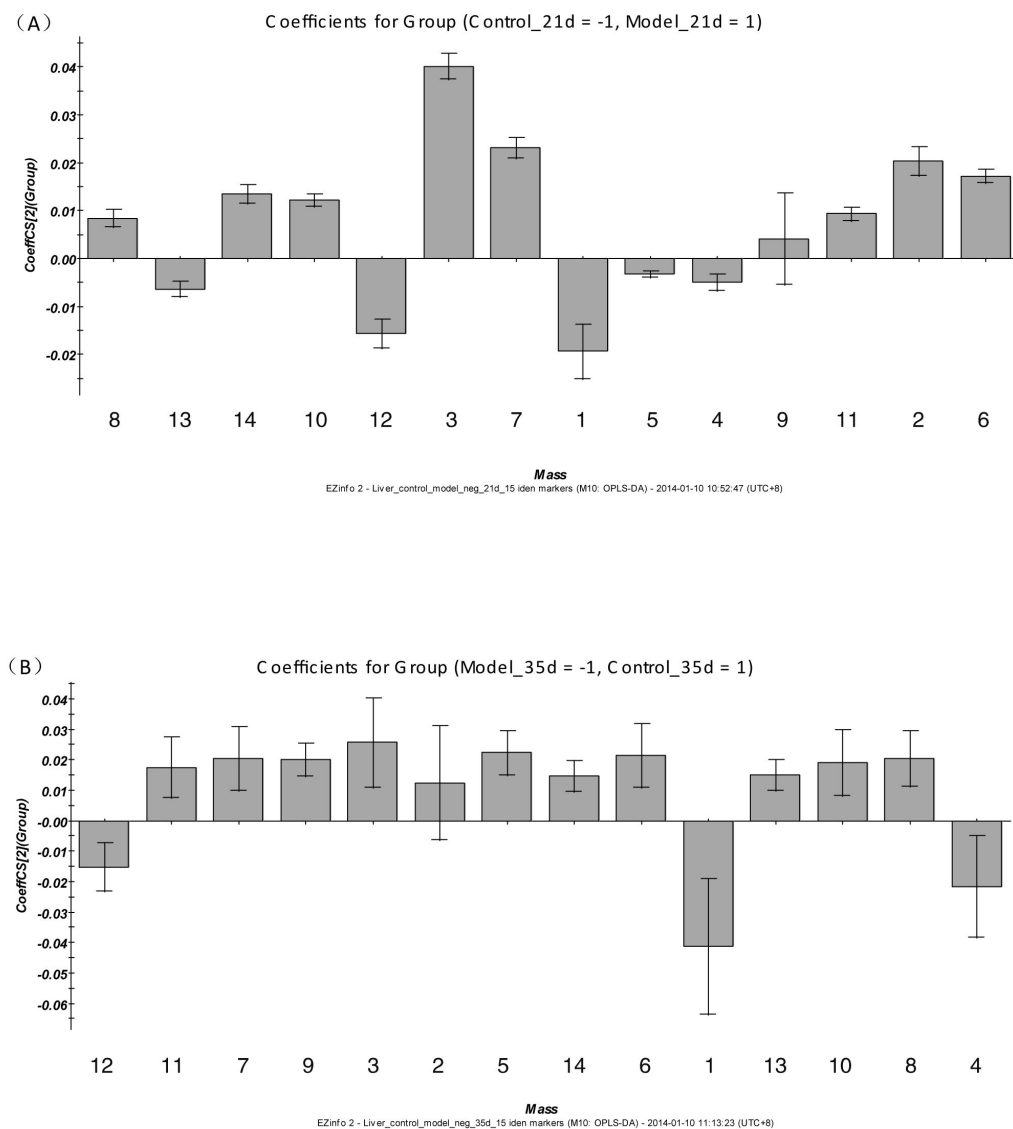


Figure 10. OPLS-DA loading plot in positive ion mode from the control group and the model group on the 21st day (A) and the 35th day (B). The loading plots represent the metabolites that are quantitatively higher or lower in the model group compared with the control group.

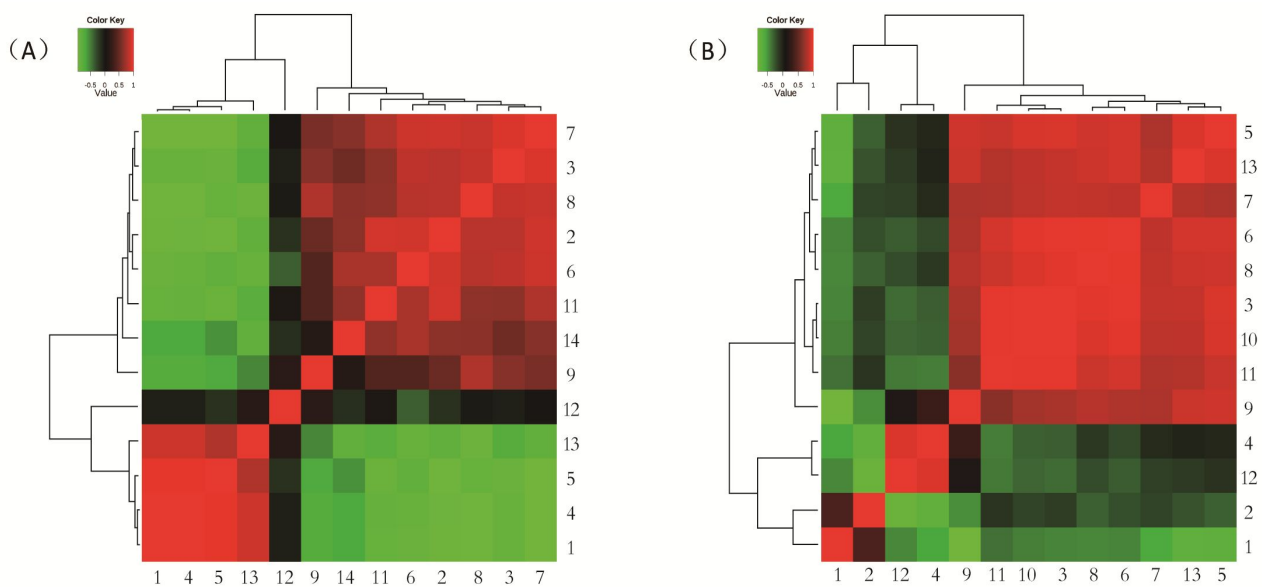


Figure 11. Correlation analysis of the differential metabolites on the 21st day (A) and the 35th say (B) are marked on the S-plots. The numbers correspond with Tables 1 and 2.

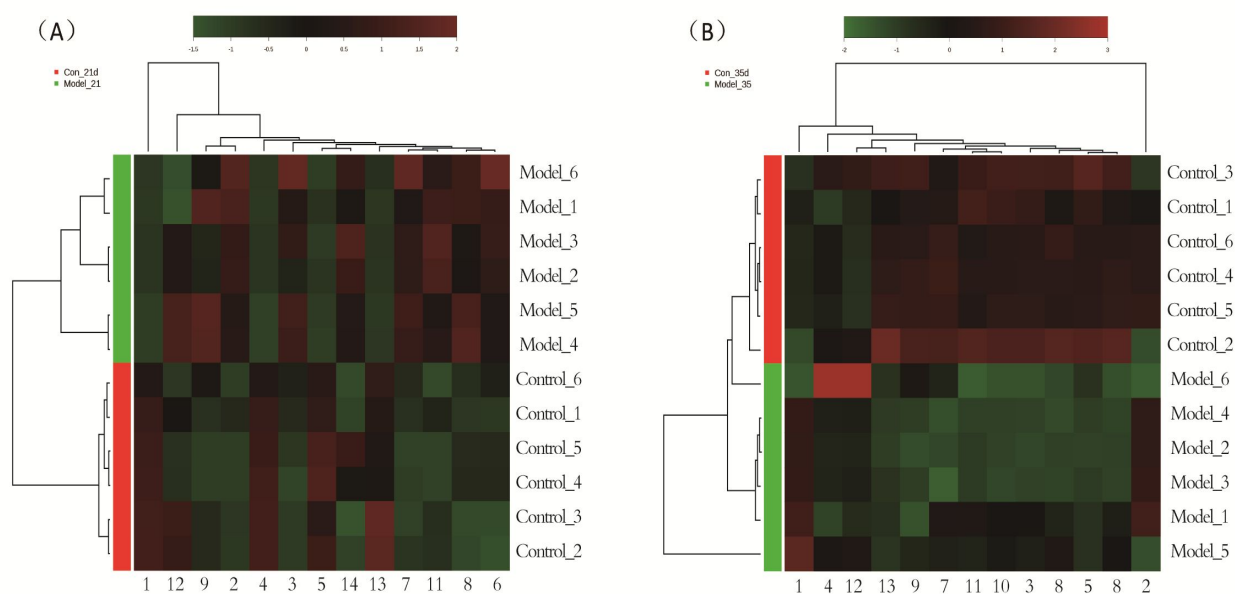


Figure 12. Heat maps for liver metabolites on the 21st day (A) and the 35th day (B). The color of each section is proportional to the significance of the change in metabolites (red, up-regulated; green, down-regulated).

Rows: samples; columns: metabolites. The numbers correspond with Tables 1 and 2.